Cerebral Vascular Atlas Generation for Anatomical Knowledge Modeling and Segmentation Purpose

N. Passat[1,2], C. Ronse[1], J. Baruthio[2], J.-P. Armspach[2], C. Maillot[3]

[1]LSIIT, Laboratoire des Sciences de l'Image, de l'Informatique et de la Télédétection (UMR 7005 CNRS/ULP)
[2]IPB, Institut de Physique Biologique (UMR 7004 CNRS/ULP)
[3]Institut d'Anatomie Normale de l'Hôpital Civil de Strasbourg

Purpose

Magnetic resonance angiography (MRA) is a family of non-invasive image acquisition processes providing 3D data of the flowing blood. Indeed, the availability of precise information about brain vascular networks is fundamental for planning and performing neurosurgical procedures, but also for detecting pathologies such as aneurysms and stenoses. Many vessel segmentation methods have been proposed during the last 15 years. Recently, a new family of segmentation algorithms [1] has been studied, involving high level anatomical knowledge. These algorithms are based on the assumption that a priori knowledge concerning the vessels and their relations to other brain structures can be used to guide classical segmentation tools. This kind of strategy requires an accurate way to model and store such anatomical information. A common way generally consists in using atlases. Nevertheless, since vessels are structures exhibiting a high variability, vascular atlas creation is a real challenge. We propose here a method to create such atlases (essentially devoted to vessel segmentation purpose) from a PC-MRA database. This method is composed of four successive steps: segmentation, quantitative analysis (determining vessels centerline and size), non-rigid registration of the different images on a same reference, and fusion of these registered images into a single one.

Background

Magnetic Resonance Angiography

Magnetic Resonance Angiography (MRA) provides non invasive 3D MR techniques enabling to visualize vascular structures by detecting the flowing blood signal. Among these techniques, Phase-Contrast MRA (PC MRA), allows to generate two different images in only one acquisition. The first data, named magnitude image, contains anatomical, but no vascular information, like a classical T1 MRI. The second data, named phase image, is obtained by only conserving the signal of moving structures. Then, it only contains the flowing blood signal, plus noise and artifacts.
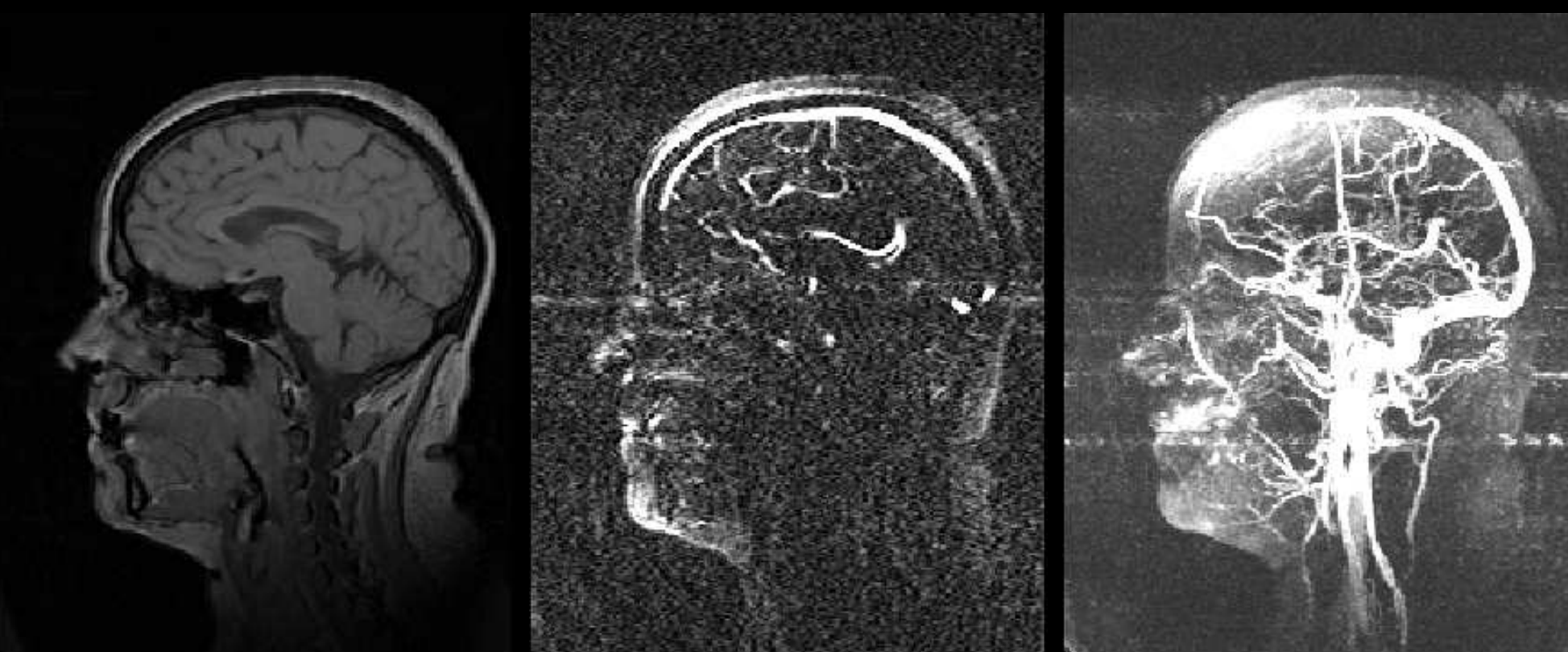
From left to right: PC MRA magnitude image (sagittal slice), PC MRA phase image (sagittal slice), PC MRA phase image (MIP visualization).

Definitions and notations

A PC-MRA data is denoted by p while a set of PC-MRA is denoted by P. The magnitude image (resp. phase image) associated to p is denoted by p_{mag} (resp. p_{pha}). These images can be defined as functions:

$$p_\alpha : [0, d_x - 1] \times [0, d_y - 1] \times [0, d_z - 1] \to \mathbb{N}$$
$$(x, y, z) \mapsto v ,$$

where d_x, d_y, d_z are the dimensions of p, $\alpha = mag$ or pha and v is the gray-level value of the image at the current point. The set $[0, d_x - 1] \times [0, d_y - 1] \times [0, d_z - 1]$ is denoted by I, and an element $(x, y, z) \in I$ will be denoted by $\mathbf{x}$.

Method

Input and output

The method takes as input a PC-MRA database $P = \{p^i\}_{i=0}^{n-1}$ of arbitrary size n and a PC-MRA magnitude image p_{mag}^{ref} used as a reference image for the registration step (p_{mag}^{ref} can be chosen in P). It provides as output a vascular atlas $\mathcal{A}$ defined by:

$$\mathcal{A} : I \to [0, 1] \times \mathcal{P}(\mathbb{R}^+) \times \mathcal{P}([0, \pi[\times[0, \pi[)$$
$$\mathbf{x} \mapsto (\mathcal{A}^d(\mathbf{x}), \mathcal{A}^t(\mathbf{x}), \mathcal{A}^o(\mathbf{x})) = (d, t, o) ,$$

where $\mathcal{P}(X) = \{x \mid x \subseteq X\}$ stands for the set of all subsets of a set X, and (d, t, o) represents the probability to find a vessel (d), the possible diameters of a vessel (t), and the set of its possible orientations (o) at the current position $\mathbf{x}$.
This atlas can also be modeled by the following function:

$$\mathcal{A}' : I \to \mathbb{R}^7$$
$$\mathbf{x} \mapsto (d, a, \sigma_a, \theta, \sigma_\theta, \phi, \sigma_\phi)(\mathbf{x}) ,$$

which enables to store it in a simple way and to easily recover any useful information it contains.

Algorithm

Segmentation [2] The segmentation step takes as input $P = \{p^i\}_{i=0}^{n-1}$ and computes the segmentation of p^i for $i = 0$ to $n - 1$:

$$p_{seg}^i : I \to \{0, 1\}$$
$$\mathbf{x} \mapsto d .$$

Quantitative analysis [3] This step takes as input $P = \{p_{seg}^i\}_{i=0}^{n-1}$ and computes diameter (p_{thi}^i) and orientation (p_{ske}^i) images:

$$p_{thi}^i : I \to \mathbb{R}^+$$
$$\mathbf{x} \mapsto t ,$$

$$p_{ske}^i : I \to [0, \pi[\times[0, \pi[$$
$$\mathbf{x} \mapsto (p_{ske,\theta}^i(\mathbf{x}), p_{ske,\phi}^i(\mathbf{x})) = o .$$

Data provided by the first two steps of the method. From left to right: p_{seg}^i, p_{ske}^i, p_{thi}^i.

Non-rigid registration [4] For all $p_{mag}^i \in P$, the PC-MRA magnitude image p_{mag}^i is registered on the reference magnitude image p_{mag}^{ref}. This registration provides a 3D deformation field D^i. Then for any $\mathbf{x} \in I$, $p^i(\mathbf{x})$ is assumed to be equal to $p_{mag}^{ref}(D^i(\mathbf{x}))$, from an anatomical point of view.
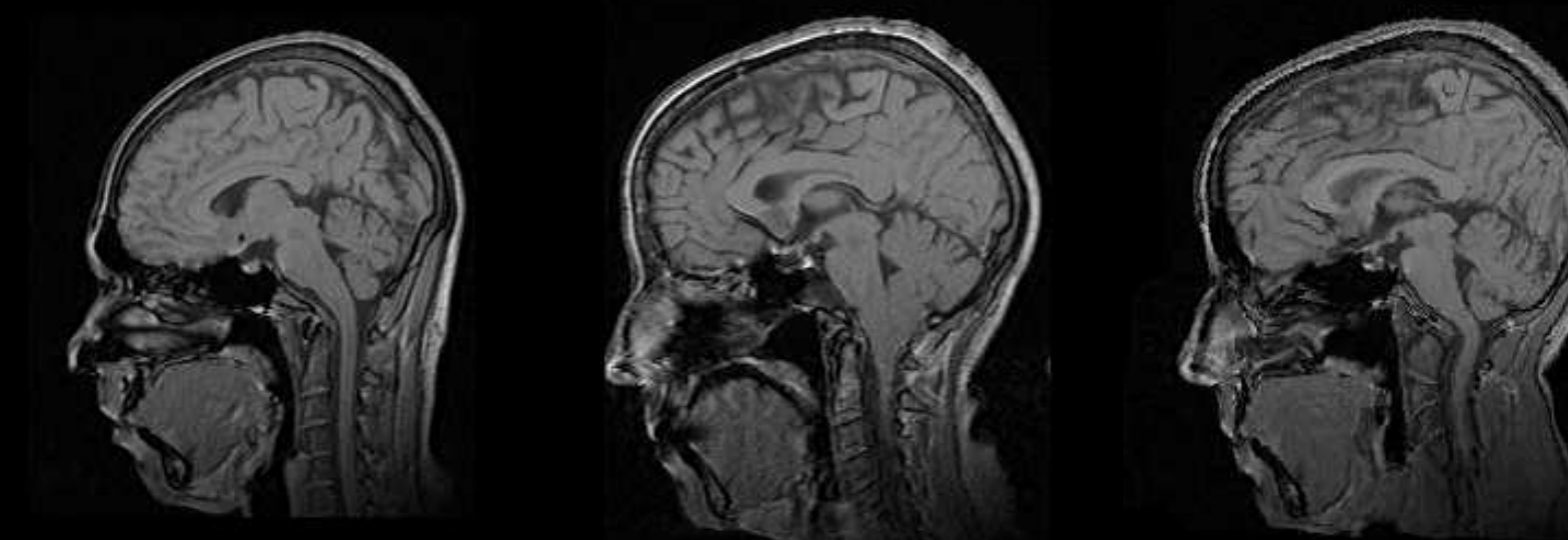
Example of non rigid registration. From left to right: source image, target image registered image.

Data fusion The first part of the atlas (vascular density):

$$\mathcal{A}^d : I \to [0, 1]$$
$$\mathbf{x} \mapsto d ,$$

is defined by:

$$\forall \mathbf{x} \in I, \mathcal{A}^d(\mathbf{x}) = \frac{1}{n} \sum_{i=0}^{n-1} p_{seg}^i((D^i)^{-1}(\mathbf{x})).$$

The second part of the atlas (vessel diameters):

$$\mathcal{A}^t : I \to \mathcal{P}(\mathbb{R}^+)$$
$$\mathbf{x} \mapsto t ,$$

is defined by:

$$\forall \mathbf{x} \in I, \mathcal{A}^t(\mathbf{x}) = [\max\{0, a(\mathbf{x}) - \sigma_a(\mathbf{x})\}, a(\mathbf{x}) + \sigma_a(\mathbf{x})],$$

where:

$$a(\mathbf{x}) = \begin{cases} 0 & \text{if } N(\mathbf{x}) = \emptyset \\ \frac{1}{\#N(\mathbf{x})} \sum_{i \in N(\mathbf{x})} p_{thi}^i((D^i)^{-1}(\mathbf{x})) & \text{otherwise} \end{cases} ,$$

with:

$$N(\mathbf{x}) = \{i \in [0, n - 1] \mid p_{seg}^i((D^i)^{-1}(\mathbf{x})) = 1\},$$

and σ_a standing for the standard deviation associated to the value a.
The last part of the atlas (vessel orientation):

$$\mathcal{A}^o : I \to \mathcal{P}([0, \pi[\times[0, \pi[)$$
$$\mathbf{x} \mapsto o ,$$

is defined by:

$$\forall \mathbf{x} \in I, \mathcal{A}^o(\mathbf{x}) = \Theta(\mathbf{x}) \times \Phi(\mathbf{x}),$$

where:

$$\Theta(\mathbf{x}) = \begin{cases} \emptyset & \text{if } N(\mathbf{x}) = \emptyset \\ [0, \pi[& \text{if } N(\mathbf{x}) \neq \emptyset \text{ and } \sigma_\theta(\mathbf{x}) \geq \pi/4 \\ [\theta(\mathbf{x}) - \sigma_\theta(\mathbf{x}), \theta(\mathbf{x}) + \sigma_\theta(\mathbf{x})] \pmod \pi & \text{otherwise} \end{cases} ,$$

$$\Phi(\mathbf{x}) = \begin{cases} \emptyset & \text{if } N(\mathbf{x}) = \emptyset \\ [0, \pi[& \text{if } N(\mathbf{x}) \neq \emptyset \text{ and } \sigma_\phi(\mathbf{x}) \geq \pi/4 \\ [\phi(\mathbf{x}) - \sigma_\phi(\mathbf{x}), \phi(\mathbf{x}) + \sigma_\phi(\mathbf{x})] \pmod \pi & \text{otherwise} \end{cases} ,$$

with:

$$\theta(\mathbf{x}) = \sum_{i \in N(\mathbf{x})} \frac{1}{\#N(\mathbf{x})} p_{ske,\theta}^i((D^i)^{-1}(\mathbf{x})),$$

$$\phi(\mathbf{x}) = \sum_{i \in N(\mathbf{x})} \frac{1}{\#N(\mathbf{x})} p_{ske,\phi}^i((D^i)^{-1}(\mathbf{x})),$$

and $\sigma_\theta(\mathbf{x})$ (resp. $\sigma_\phi(\mathbf{x})$) standing for the standard deviation associated to $\theta(\mathbf{x})$ (resp. $\phi(\mathbf{x})$).

Experiments and Results

Experiments

Software Method implemented in C++ (using the ImLib3D [5] open source C++ library) and integrated in the Medimax image processing software platform.
Hardware 3 GHz Pentium IV processor, 2 GB of memory.
Imaging The 18 MRA (dimensions varying between $256^2 \times 150$ and $256^2 \times 180$ voxels) used for validation have been performed on a 1 Tesla whole-body scanner (Gyroscan NT/INTERA 1.0 T from Philips, gradient slope 75 T/m/s, flow encoding sequence T1FFE/PCA with a TR of 10 ms and a TE of 6.4 ms).
Computation time The successive steps of the algorithms respectively required 45, 6, and 40 minutes for each image of the database. The data fusion required 15 minutes for a 18 image database.

Results

Vascular density

Probability	# voxels	Ratio
$p = 0$	9 028 698	96.18 %
$0 < p \leq 0.1$	209 718	2.23 %
$0.1 < p \leq 0.2$	87 390	0.93 %
$0.2 < p \leq 0.3$	27 031	0.29 %
$0.3 < p \leq 0.4$	13 192	0.14 %
$0.4 < p \leq 0.5$	7 092	0.08 %
$0.5 < p$	6 719	0.07 %
$p \neq 0$	351 142	3.74 %

Distribution of the probability (p) to find a vascular structure. First column: values of p; second and third columns: number and ratio of voxels $\mathbf{x}$ such as $\mathcal{A}^d(\mathbf{x}) = p$.
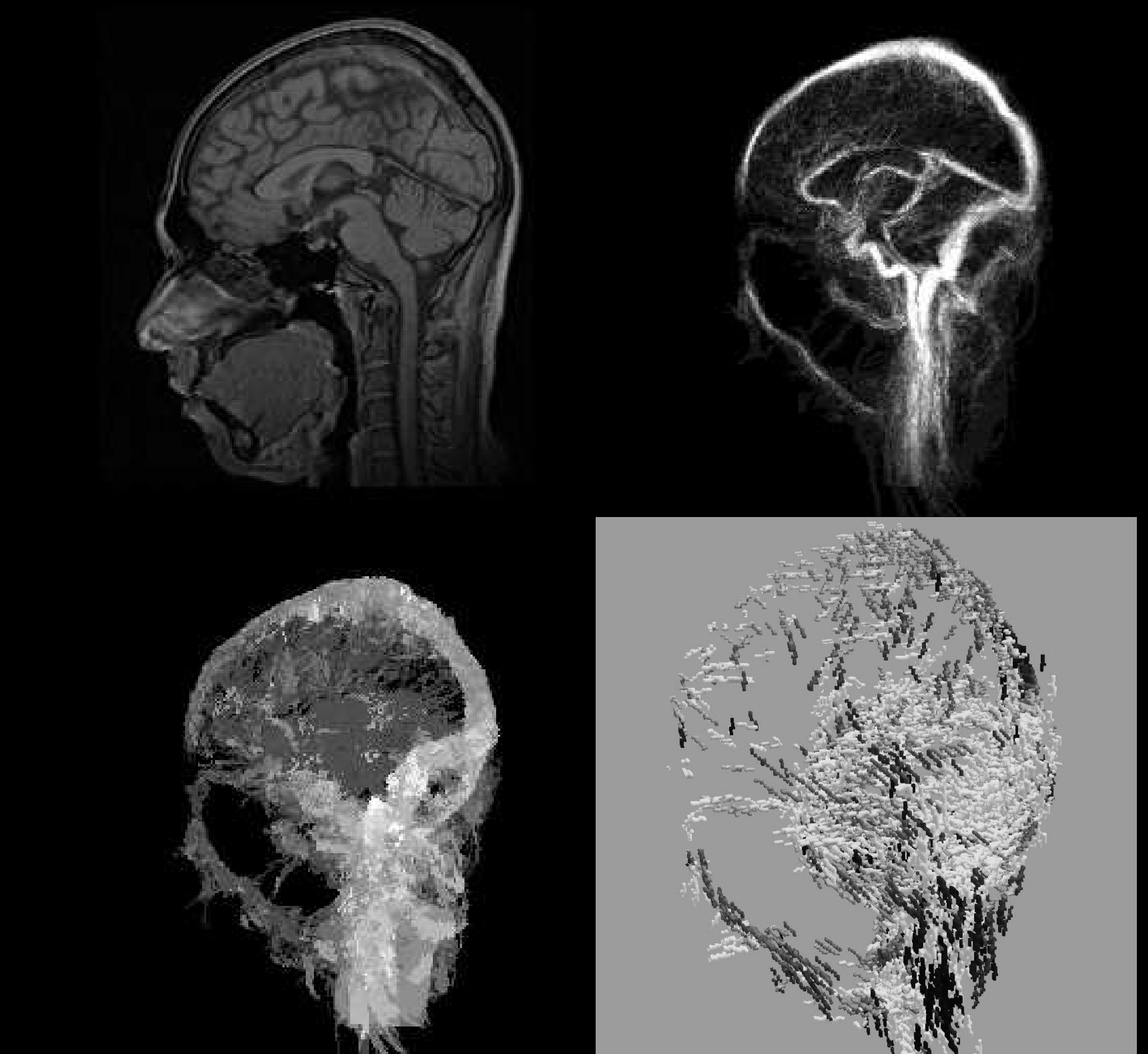
Vessel diameters

Diameter (mm)	# voxels	Ratio
$0 < t \leq 1.0$	5 066	1.44 %
$1.0 < t \leq 2.0$	80 282	22.86 %
$2.0 < t \leq 3.0$	111 372	31.72 %
$3.0 < t \leq 4.0$	80 139	22.82 %
$4.0 < t \leq 5.0$	56 547	16.10 %
$5.0 < t \leq 6.0$	14 411	4.10 %
$6.0 < t$	3 121	0.89 %

Distribution of the average diameters of the vessels in the vascular part of the image (part presenting non zero values for $\mathcal{A}^d$). First column: average diameter (t); second and third columns: number and ratio of voxels $\mathbf{x}$ such as $a(\mathbf{x}) = t$.

Vessel orientations

Orientation	θ		ϕ	
(rad.)	# voxels	Ratio	# voxels	Ratio
Undefined	253 978	72.33 %	261 496	74.48 %
$[0, \pi/6[$	3 540	1.01 %	7 298	2.08 %
$[\pi/6, \pi/3[$	14 931	4.25 %	24 873	7.08 %
$[\pi/3, \pi/2[$	31 174	8.88 %	21 669	6.17 %
$[\pi/2, 2\pi/3[$	27 679	7.88 %	16 898	4.81 %
$[2\pi/3, 5\pi/6[$	13 597	3.87 %	14 685	4.18 %
$[5\pi/6, \pi]$	6 243	1.78 %	4 223	1.20 %

Distribution of the orientation of the vessels in the vascular part of the image (part presenting non zero values for $\mathcal{A}^d$). First column: values of θ or ϕ; second and third (resp. fourth and fifth) columns: number and ratio of voxels presenting the current orientation according to θ (resp. ϕ).

Visualization of elements of the processed atlas. Upper-left image: Reference magnitude image (p_{mag}^{ref}). Upper-right image: probability to find a vessel ($\mathcal{A}^d$), visualized as a MIP of the sagittal slices. Lower-left: average vessel diameters (part a of $\mathcal{A}^t$), visualized as a MIP of the sagittal slices. Lower-right: 3D visualization of a part of the orientation image (lines oriented according to θ and ϕ); the gray level linearly depends on the θ value.

References

[1] N. Passat, C. Ronse, J. Baruthio, J.-P. Armspach. Automatic Parameterization of Grey-Level Hit-or-Miss Operators for Brain Vessel Segmentation. 2005 *IEEE International Conference on Acoustics, Speech, and Signal Processing - ICASSP 2005*, Part II:737–740, 2005.
[2] N. Passat, C. Ronse, J. Baruthio, J.-P. Armspach, C. Maillot, C. Jahn. Region-Growing Segmentation of Brain Vessels: An Atlas-Based Automatic Approach. *Journal of Magnetic Resonance Imaging* (to appear).
[3] D. Chillet, N. Passat, M.-A. Jacob-Du Col, J. Baruthio. Thickness Estimation of Discrete Tree-Like Tubular Objects. Application to Vessel Quantification. *Scandinavian Conference on Image Analysis - SCIA'05* (to appear).
[4] V. Noblet, C. Heinrich, F. Heitz, J.-P. Armspach. A Topology Preserving Non-Rigid Registration Method Using a Symmetric Similarity Function - Application to 3-D Brain Images. *European Conference on Computer Vision - ECCV 2004*, in Lecture Notes in Computer Science, **3023**:546–557, 2004.
[5] M. Bosc, T. Vik, J.-P. Armspach, F. Heitz. ImLib3D: An Efficient, Open Source, Medical Image Processing Framework in C++. *Medical Image Computing and Computer-Assisted Intervention - MICCAI'03*, in Lecture Notes in Computer Science, **2879**:981–982, 2003.

N. Passat (mail: passat@dpt-info.u-strasbg.fr; Web: https://dpt-info.u-strasbg.fr/~passat)
C. Ronse (mail: cronse@dpt-info.u-strasbg.fr; Web: http://arthur.u-strasbg.fr/~ronse)
J. Baruthio (mail: baruthio@ipb.u-strasbg.fr)
J.P. Armspach (mail: armspach@ipb.u-strasbg.fr; Web: http://alsace.u-strasbg.fr/ipb/staff/armspach)

LSIIT: http://lsiit.u-strasbg.fr
IPB: http://alsace.u-strasbg.fr/ipb

The Medimax image processing software platform is available at http://www-ipb.u-strasbg.fr.
The ImLib3D C++ library is available at http://imlib3d.sourceforge.net.